

Burkitt-like lymphoma with 11q aberration: a germinal center-derived lymphoma genetically unrelated to Burkitt lymphoma

Blanca Gonzalez-Farre,^{1,2,3*} Joan Enric Ramis-Zaldivar,^{2,3*} Julia Salmeron-Villalobos,² Olga Balagué,^{1,2,3} Verónica Celis,⁴ Jaime Verdu-Amoros,⁵ Ferran Nadeu,^{2,3} Constantino Sábado,⁶ Antonio Ferrández,⁷ Marta Garrido,⁸ Federico García-Bragado,⁹ María Dolores de la Maya,¹⁰ José Manuel Vagace,¹⁰ Carlos Manuel Panizo,¹¹ Itziar Astigarraga,¹² Mara Andrés,¹³ Elaine S. Jaffe,¹⁴ Elias Campo^{1,2,3*} and Itziar Salaverria^{2,3*}

¹Hematopathology Unit, Hospital Clínic de Barcelona, University of Barcelona, Barcelona, Spain; ²Institut d'Investigacions Biomèdiques August Pi i Sunyer (IDIBAPS), Barcelona, Spain; ³Centro de Investigación Biomédica en Red de Cáncer (CIBERONC), Madrid, Spain; ⁴Pediatric Oncology Department, Hospital Sant Joan de Déu, Esplugues de Llobregat, Spain; ⁵Pediatric Oncology Department, Hospital Clínico Universitario de Valencia, Valencia, Spain; ⁶Pediatric Oncology Department, Hospital Universitari Vall d'Hebron, Barcelona, Spain; ⁷Pathology Department, Hospital Clínic de Valencia, Valencia, Spain; ⁸Pathology Department, Hospital Universitari Vall d'Hebron, Barcelona, Spain; ⁹Pathology Department, Complejo Hospitalario de Navarra, Pamplona, Spain; ¹⁰Pediatric Hematology Department, Hospital Materno Infantil de Badajoz, Badajoz, Spain; ¹¹Department of Hematology, Clínica Universidad de Navarra and Instituto de Investigación Sanitaria de Navarra (IdiSNA), Pamplona, Spain; ¹²Pediatrics Department, Hospital Universitario Cruces, IIS Biocruces Bizkaia, UPV/EHU, Barakaldo, Spain; ¹³Pediatric Oncology Department, Hospital La Fe, Valencia, Spain and ¹⁴Hematopathology Section, Laboratory of Pathology, National Cancer Institute, National Institutes of Health, Bethesda, MD, USA

*BGF, JERZ, EC and IS contributed equally to this work.

©2019 Ferrata Storti Foundation. This is an open-access paper. doi:10.3324/haematol.2018.207928

Received: October 5, 2018.

Accepted: February 7, 2019.

Pre-published: February 7, 2019.

Correspondence: ITZIAR SALAVERRIA - isalaver@clinic.cat

Supplementary Material

Burkitt-like lymphoma with 11q aberration: A germinal center derived lymphoma genetically unrelated to Burkitt lymphoma

Gonzalez-Farre & Ramis-Zaldivar et al

Supplementary Methods.....	Page 3
Supplementary Results.....	Page 5
Supplementary Figures.....	Page 7
Supplementary Tables.....	Page 16
Supplementary References.....	Page 30

Supplementary Methods

Copy number analysis

DNAs were hybridized on Oncoscan FFPE or SNP array platform (ThermoFisher Scientific, Waltham, MA). Gains and losses and copy-number neutral loss of heterozygosity (CNN-LOH) regions were evaluated and visually inspected using Nexus Biodiscovery version 9.0 software (Biodiscovery, Hawthorne, CA). Human reference genome was GRCh37/hg19. The copy number alterations (CNAs) with minimum size of 100 kb and CNN-LOH larger than 5 Mb were considered informative. Physiological deletions of the immunoglobulin loci were excluded from the analysis. T-cell receptor locus deletions were also excluded, most probably representing physiological deletions of accompanying reactive T cells. Copy number data are deposited at GEO database GSE116527. Published CN data on *MYC*-positive BL¹ were reanalyzed.

Library preparation SureSelect XT and Targeted sequencing approach

DNA and RNA were extracted using standard protocols from formalin fixed paraffin embedded material in 12 and frozen tissue in 3 cases (Qiagen, Hilden, Germany). A total of 100ng of genomic DNA was sheared using the Covaris S220 focused-ultrasonicator (Covaris, Woburn, MA) to a target peak size of 150–200 bp. Library preparation were performed using SureSelectXT Custom Capture Library baits as described in SureSelectXT Target Enrichment System protocol (Agilent Technologies, Santa Clara, CA). For amplification of the post capture libraries, 10 to 13 cycles were performed depending on the initial sample quality. The libraries were qualified using the Bioanalyzer HS (Agilent technologies), quantified with the KAPA Library Quantification Kit (Kapa Biosystems, Wilmington, Massachusetts) and sequenced in a MiSeq instrument (Illumina, San Diego, CA) in a paired-end run of 150 bp. The average sequencing coverage of 10 Burkitt-like lymphoma with 11q (BLL-11q) cases across

regions was 478x (range 97-1229) and over 93% of the targeted regions were covered by at least 100 reads. (**Supplementary Figure S7**).

FASTQ files were generated by MiSeq control software and quality control of the raw data was performed using the FastQC tool (<https://www.bioinformatics.babraham.ac.uk/projects/fastqc/>). Sequencing reads were subsequently aligned to the human reference genome (GRCh37/hg19) using the Burrows-Wheeler Aligner–MEM algorithm.² Variant calling was performed using two different variant callers: Somatic Variant Caller (Illumina) and annotated using the VariantStudio software v3.0 and Mutect2 (Genome Analysis Toolkit (GATK), version 4.0.3)³ and annotated by ANNOVAR.⁴ We used Somatic Variant Caller (Illumina) with the default settings to analyze sequencing results and to call the variants. Low quality or low coverage calls (total depth <20) were excluded. For Mutect2 variants, low quality variants were also excluded using FilterMutectCalls (GATK) with default thresholds. Only variants identified by both algorithms were considered. For further analysis we excluded all synonymous and intron variants outside splicing sites (not included in the panel, with exception of intron 1 of *MYC*) and known polymorphisms described in the Single Nucleotide Polymorphism Database (dbSNP138) or ExAC database (release 2015) with more than 0.1% frequency according to the corresponding ethnicity. Finally, each variant was also inspected with the Integrative Genomics Viewer (IGV, Broad Institute, version 2.3) software to exclude artifacts.

Prediction of mutation effect

Since there was no germline DNA available, in order to select somatic variants, potential driver mutations were predicted according to previously published criteria⁵ in which the 90% of the mutations classified as functional were demonstrated to be somatic (**Supplementary Table S7**). Inclusion criteria were: 1) any variant described previously as somatic or functional on previous reports or COSMIC, 2) All truncating variants (nonsense, frameshift, splice donor or acceptor mutations; and 3) the

remaining missense variants that were predicted to be functionally deleterious using Mutation Assessor⁶ and SIFT⁷ predictors. Other predictors as Polyphen-2 (Polymorphism Phenotyping-2)⁸ and CADD (Combined Annotation Dependent Depletion)⁹ were also used.

Quantitative PCR

Gene expression levels of *MYC* and *ETS1* of 10 BLL-11q with RNA available and 12 conventional *MYC*-positive BL were investigated by real time quantitative PCR (qPCR) as described previously.¹⁰ Complementary DNA synthesis was carried out from 500 ng of total RNA and the product was amplified and quantified using TaqMan Universal PCR Master Mix no AmpErase UNG (Thermo Fisher Scientific Inc.), designed primer sets, and TaqMan Gene Expression Assays for *MYC* (Hs00153408_m1) and *ETS1* (Hs00428293_m1) (Thermo Fisher Scientific Inc.).

DNA was analyzed using duplicates in a StepOne Plus Real-Time PCR System (Thermo Fisher Scientific Inc.). Relative quantification of gene expression was then analyzed with the $2^{-\Delta\Delta Ct}$ method using *B2M* (Hs00939627_m1), as the endogenous control gene, and Universal Human Reference RNA (Stratagene, Agilent Technologies, Santa Clara, CA, USA), composed of total RNA from 10 human cell lines, as the mathematical calibrator.

Supplementary Results

Morphological features of 9 *MYC*-negative, 11q-negative lymphoma cases

Among the 95 cases with an initial diagnosis of BL, atypical BL or high grade B-cell lymphoma, not otherwise specified (HGBCL,NOS) nine (9.5%) were negative for *MYC* rearrangements, using both the break-apart and the double fusion probes (only seven cases analyzed), and for the 11q alteration. After the morphological review three cases were better reclassified to diffuse large B-cell lymphoma (DLBCL). These cases were composed of a proliferation of centroblastic cells with starry sky pattern, germinal

center phenotype and very high proliferative index. One case was weakly positive for BCL2. The remaining 6 cases had HGBCL, NOS morphology, two of them with blastoid features. Four cases had a germinal center phenotype and BCL2 negativity and two cases had an activated phenotype with BCL2 positivity. All cases had a proliferative index close to 100%.

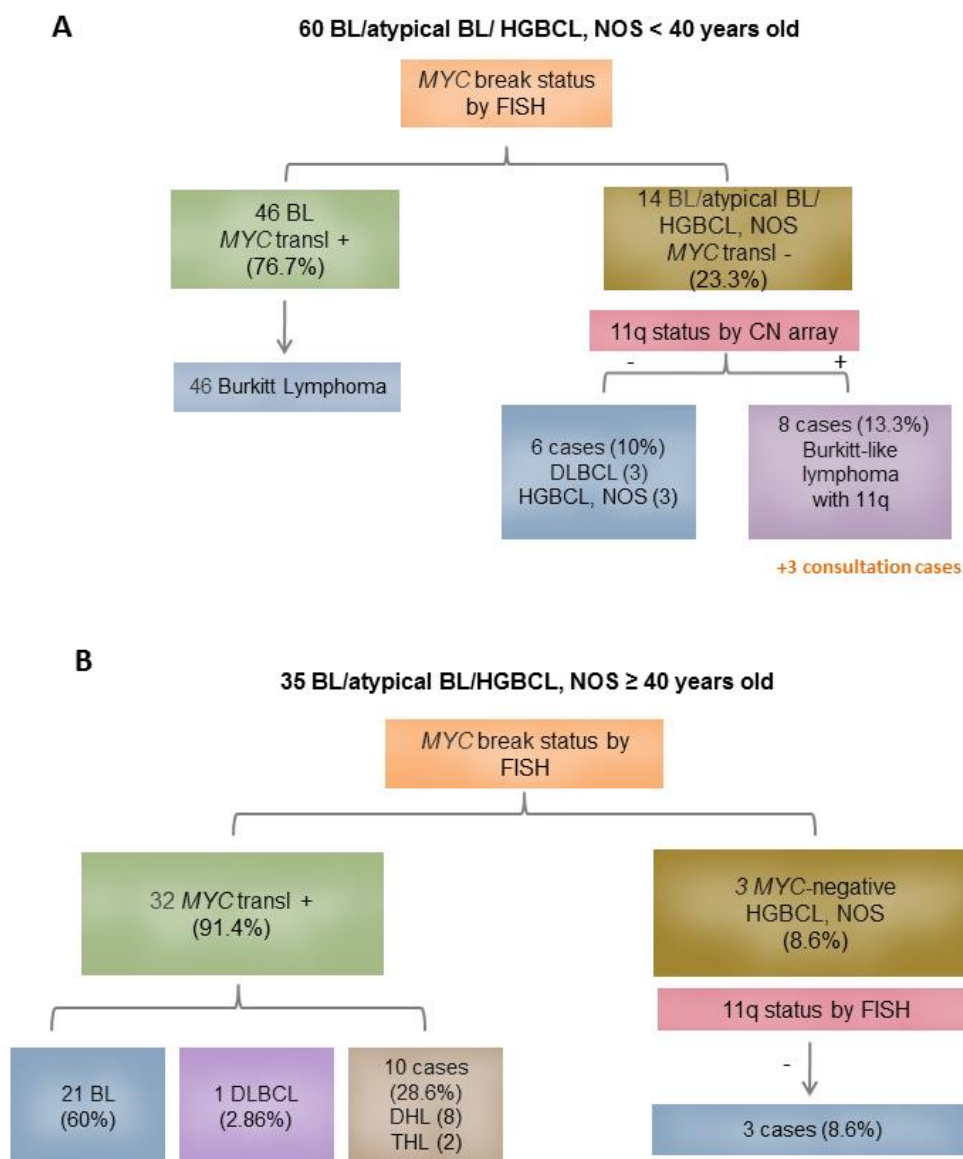
Comparison of Copy number profile of BLL-11q with other lymphoma entities

BLL-11q lymphoma had similar levels of genomic complexity as conventional *MYC*-positive BL with 7.1 vs. 6 alterations, respectively. However, gains of 5q21.3-q32 and losses of 6q12.1-q21 were virtually exclusive of BLL-11q whereas 1q gains were only seen in *MYC*-positive BL. In comparison to the two molecular DLBCL subtypes, BLL-11q cases displayed significantly lower levels of complexity than ABC and GCB-DLBCL (7.1 vs. 22 alterations in ABC and 19 alterations in GCB; both $P < 0.001$), had the specific 11q alterations and lacked gains of 2p16.1 and 7p and losses of 1p36.32 associated with GCB phenotype and losses of 6q23.3, 9p21.3 and 17p13.2 related to ABC-DLBCL.

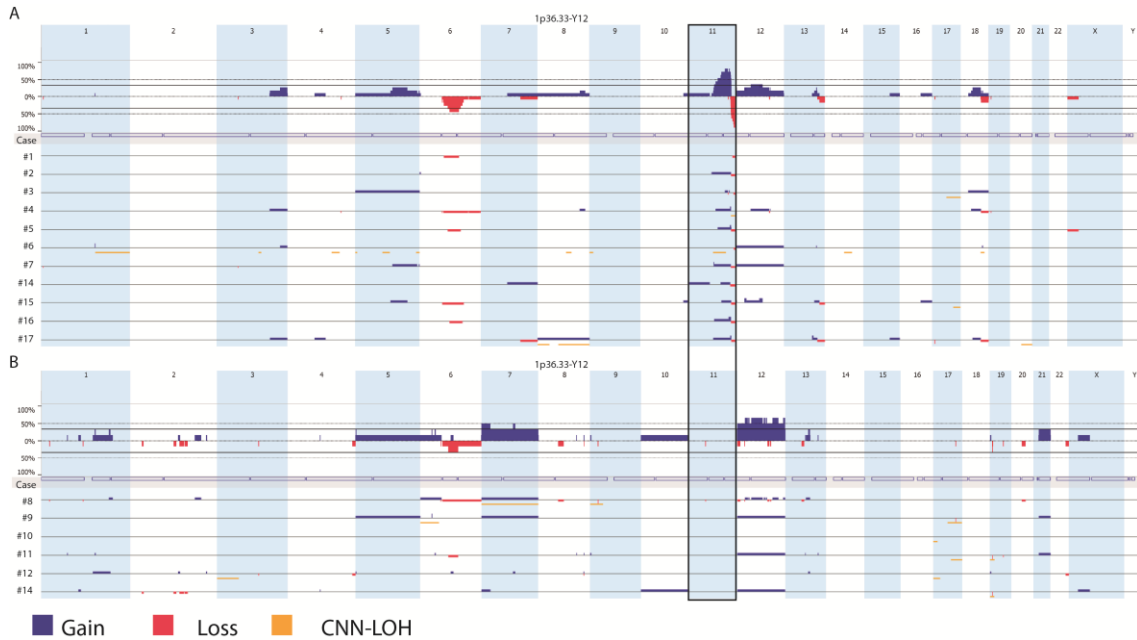
To determine the specificity of the 11q-gain/loss pattern in BLL-11q in comparison to lymphoid neoplasms other than BL and DLBCL, we screened previously published data considering both patterns of prototypical pattern of gain followed by loss or only the presence of terminal 11q24.3-q25 loss. Frequencies observed were less than 1% in all the reviewed entities including follicular lymphoma,¹¹ nodal marginal zone lymphoma,¹² chronic lymphocytic leukemia¹³ or plasma cell myeloma^{14,15} with exception of transformed follicular lymphoma¹¹ in which 16% cases, presented the 11q aberrations. These data suggest that this alteration is mainly absent in other recognized lymphoma entities and characterizes genetically BLL-11q tumors.

Supplementary Figures

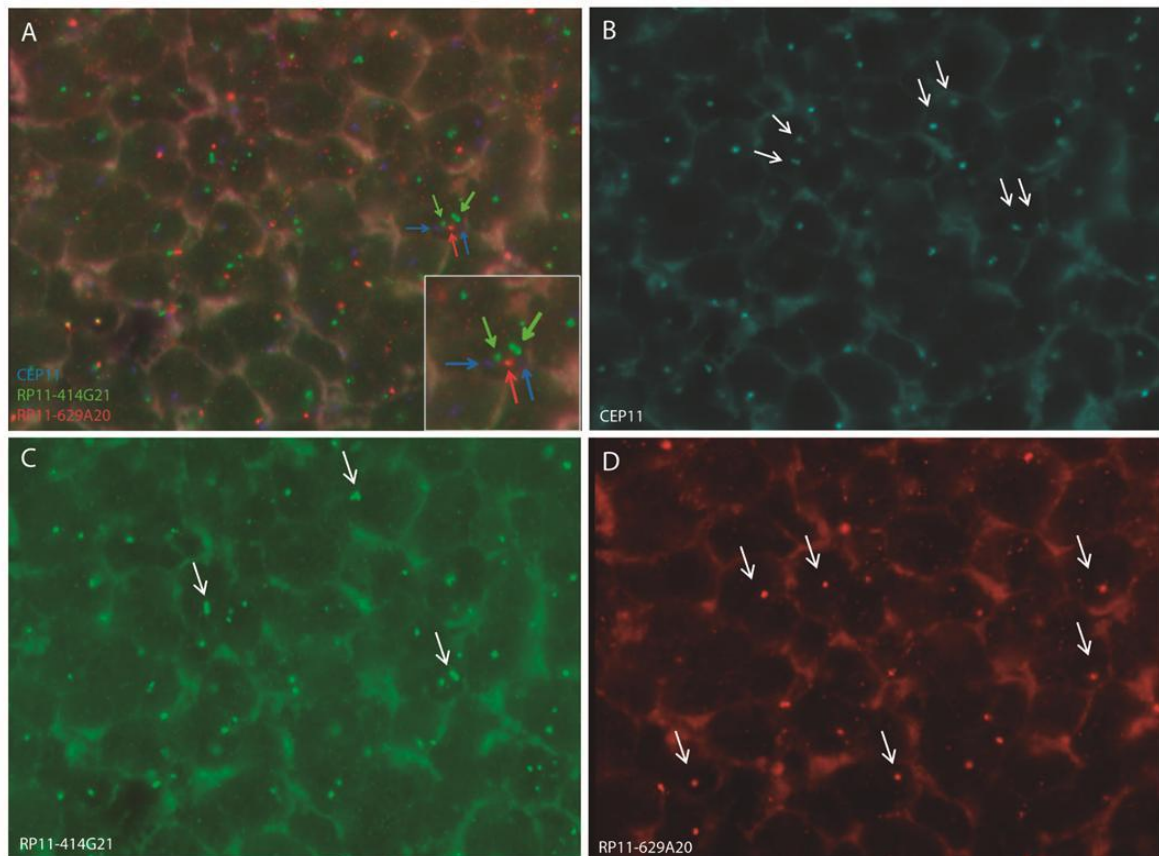
Supplementary Figure S1. Diagram of the strategy used for the identification of Burkitt-like with 11q aberration in a cohort of **(A)** 60 patients <40 years old and **(B)** 35 patients \geq 40 years old with a morphological diagnosis of Burkitt lymphoma (BL)/atypical BL and high grade B-cell lymphoma, not otherwise specified (HGBCL, NOS) according to the updated WHO Classification 2016.¹⁶ Seven out of nine cases negative for both *MYC* and 11q alterations with material available were tested by *MYC*/*IGH* double color double fusion probe, and all resulted to be negative for the fusion. Abbreviations: DLBCL, diffuse large B-cell lymphoma; DHL, double hit lymphoma; THL, triple hit lymphoma.



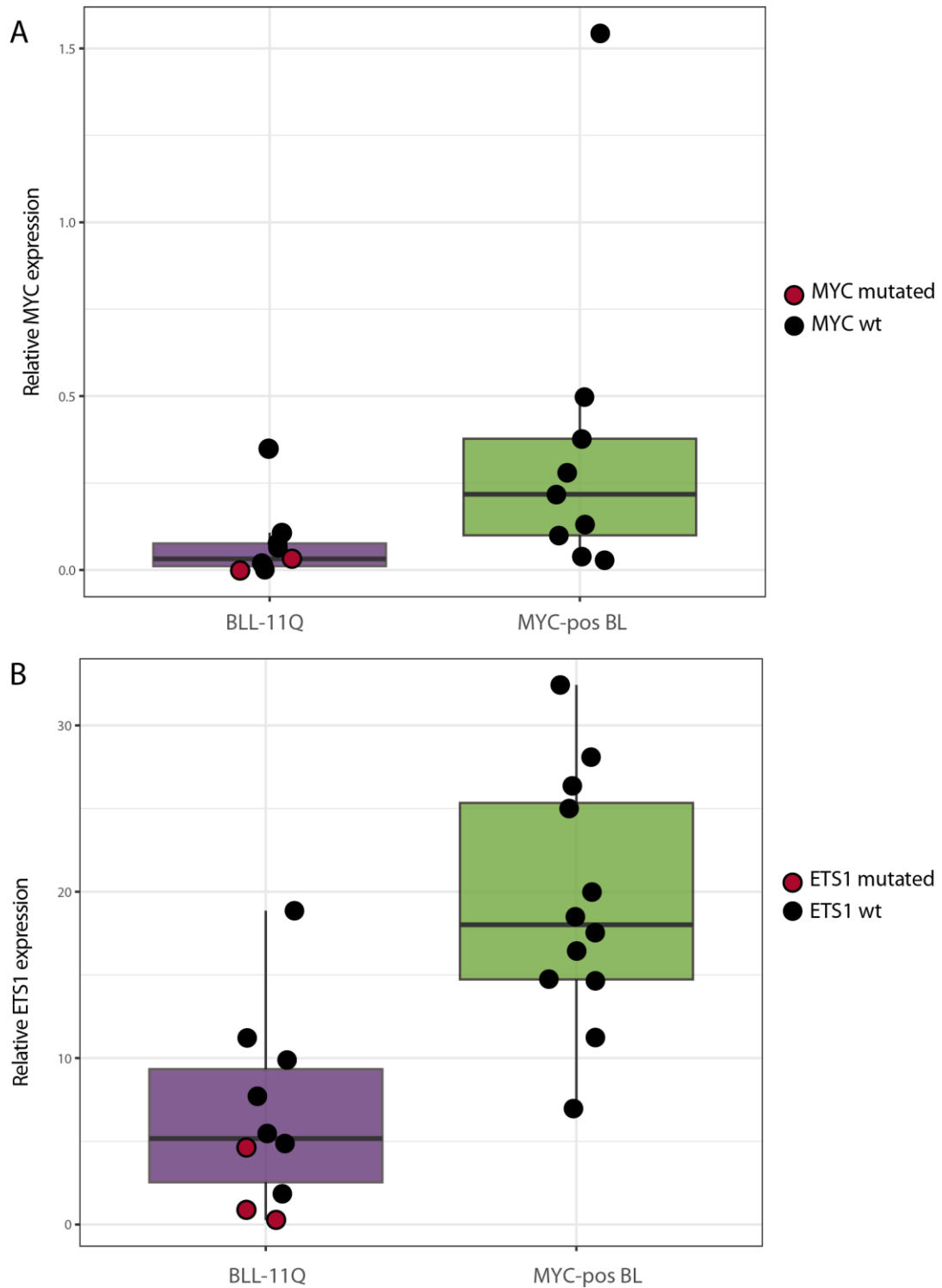
Supplementary Figure S2. Individual and integrative copy number plots of (A) eleven Burkitt-like with 11q and (B) six *MYC*-negative 11q-negative lymphoma cases. The vertical axis indicates frequency of the genomic aberration among the analyzed cases. Gains are depicted in blue, losses are depicted in red, and regions of CNN-LOH are represented in yellow.



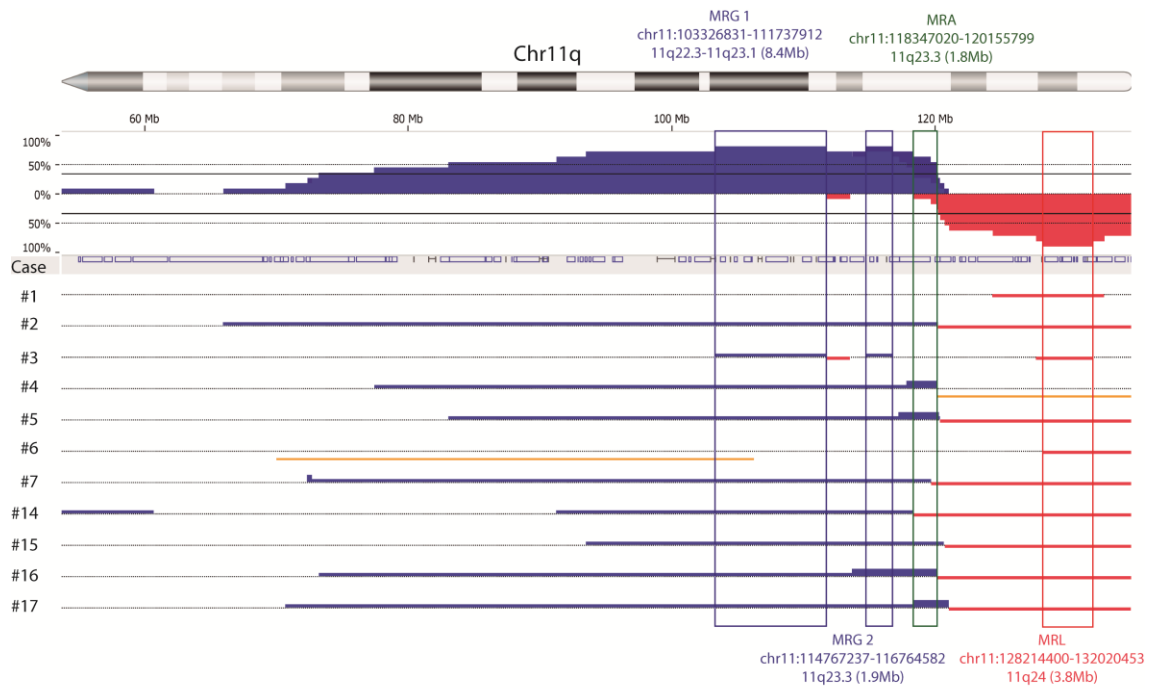
Supplementary Figure S3. Representative 11q aberration by FISH. (A) FISH image of a representative case (#17) harboring 11q aberration using a custom probe combining CEP11 (Spectrum Aqua), RP11-414G21 (Spectrum Green) and R11-629A20 (Spectrum Red) bac clones. (B) Two blue signals are observed per cell corresponding to the two chr11 centromeres, (C) the presence of three green signals per cell indicates 11q gain and (D) the presence of only one red is indicative of the 11q terminal loss.



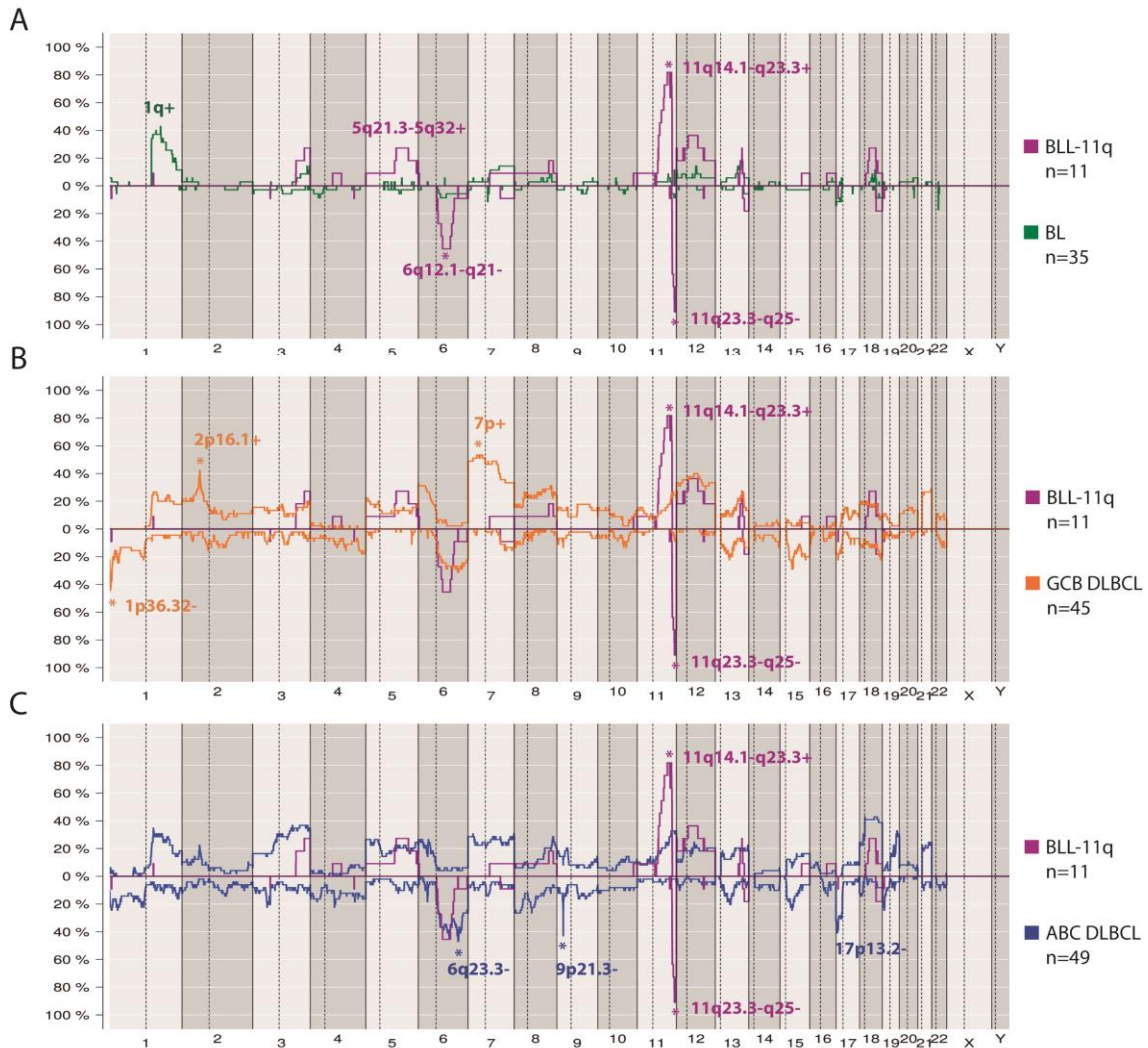
Supplementary Figure S4. *MYC* and *ETS1* RNA expression levels in BLL-11q. **(A)** Box plot of the percentage of *MYC* expression analyzed by qPCR in BLL-11q (n=9) vs. *MYC*-positive BL (n=9). **(B)** Box plot of the percentage of *ETS1* expression analyzed by qPCR in BLL-11q (n=10) vs. *MYC*-positive BL (n=12). The significance of difference was determined by t-test and Mann-Whitney test respectively.



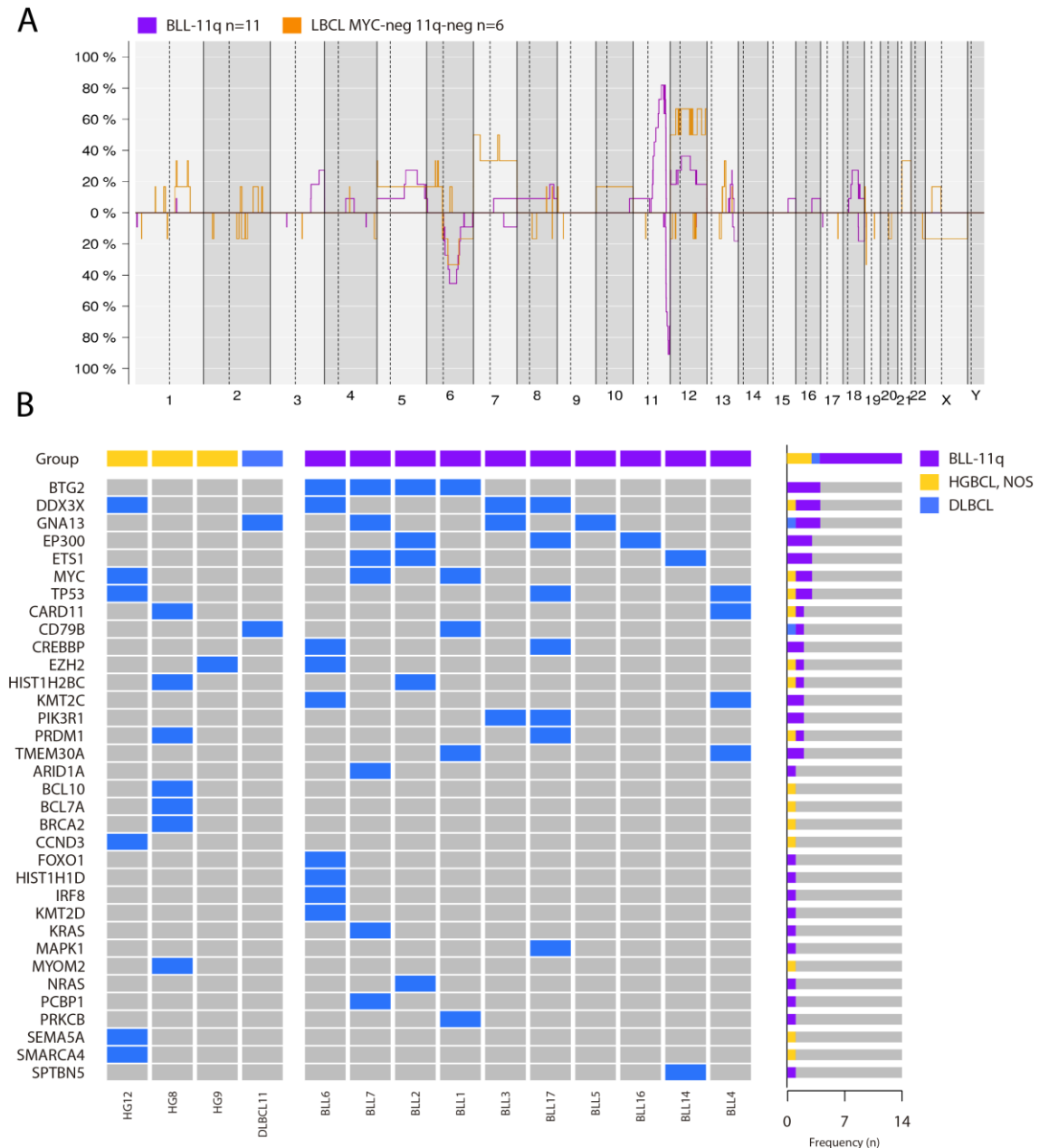
Supplementary Figure S5. Ideogram of chromosome 11q arm of 11 *MYC*-negative cases harboring 11q aberration by CN array. Gains are represented in blue, red corresponds to losses and CNN-LOH are represented in yellow. Two minimal regions of gain (MRGs) and one minimal region of loss (MRL) are pointed with blue and red boxes, respectively, and the minimal region of amplification (MRA) is indicated with the green box.



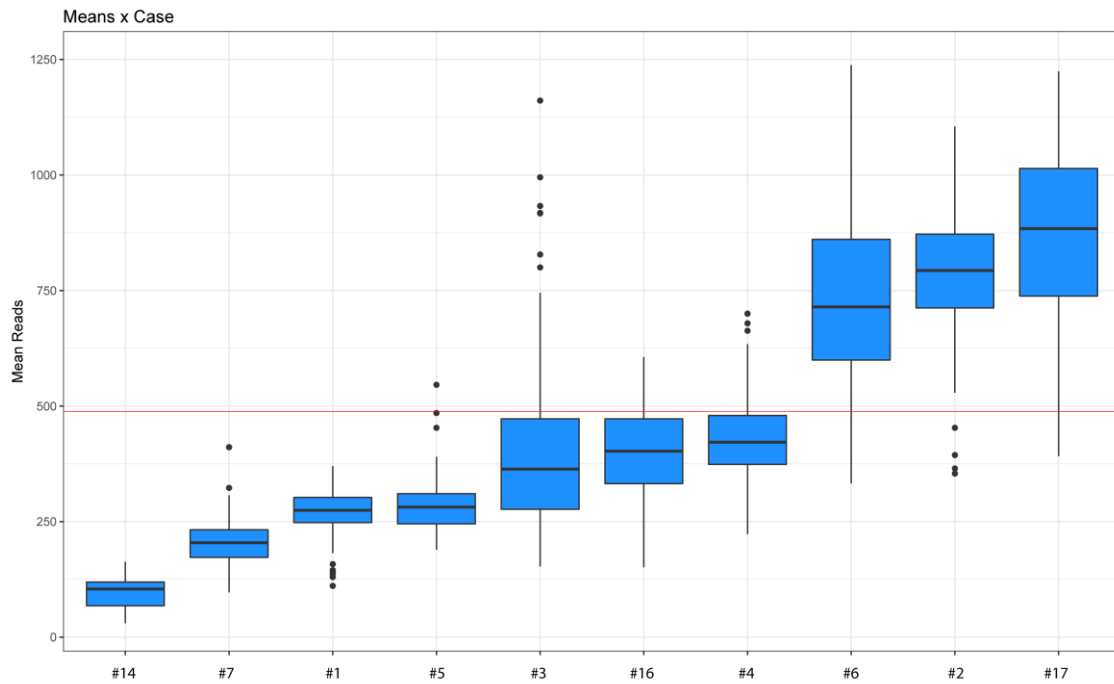
Supplementary Figure S6. Comparative plot of copy number aberrations between Burkitt-like lymphoma with 11q aberration (n=11) and **(A)** conventional *MYC*-positive Burkitt Lymphoma (n=35),¹ **(B)** GCB-Diffuse Large B-cell lymphoma (n=45)⁵ and **(C)** ABC-Diffuse Large B-cell lymphoma (n=49)⁵ X-axis depicts chromosome positions with dotted lines pointing centromeres. Y-axis indicates frequency of the genomic aberration among the analyzed cases. Significantly different regions of alterations among groups (Fisher test non-adjusted $P \leq 0.01$) are labeled with corresponding color asterisks.



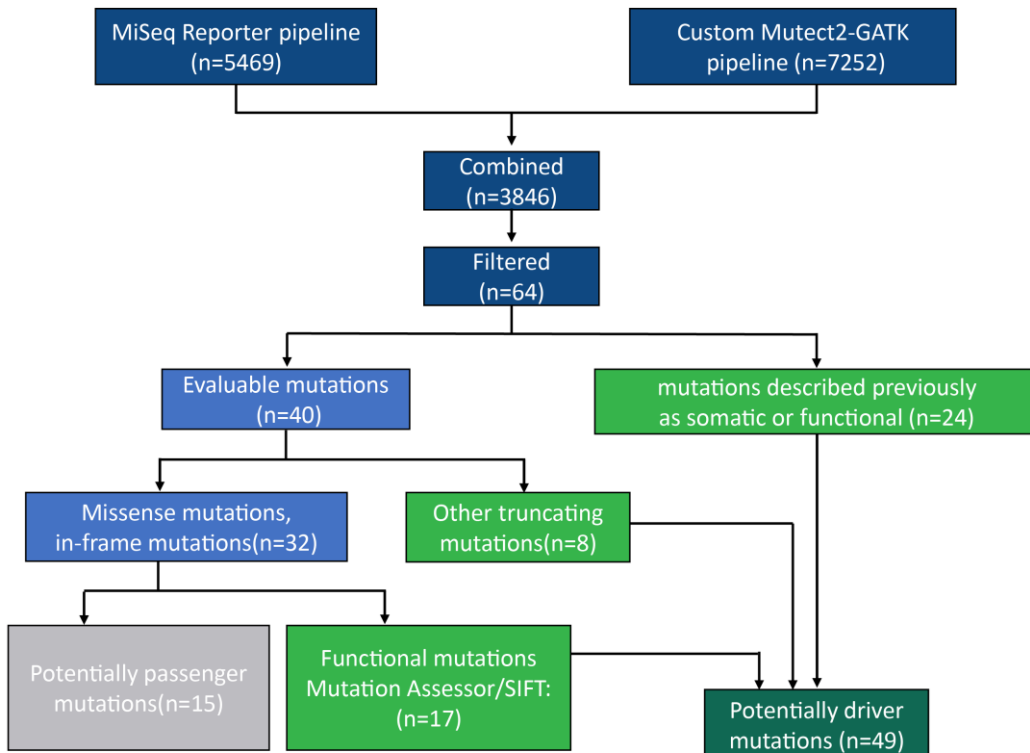
Supplementary Figure S7. (A) Comparative plot of copy number aberrations between Burkitt-like lymphoma with 11q aberration (n=11) and 6 *MYC*-negative 11q-negative cases **(B)** Mutational overview of 4 *MYC*-negative 11q negative cases in comparison with BLL with 11q aberration. The heat map shows the case specific pattern of driver mutations found by next generation sequencing. Each column represents a case and each row represents a gene. The right bar graph illustrates the mutation frequency of each gene.



Supplementary Figure S8. Mean coverage distribution per gene of the 10 BLL-11q cases analyzed by target NGS. Y-axis indicates the mean number of reads. The red line depicts the mean coverage of all 10 cases. DNA from #2, #4 and #7 BLL-11q cases were extracted from frozen tissue.



Supplementary Figure S9. NGS analysis pipeline followed to identify potential driver mutations in 10 BLL-11q samples. Two different variant callers were used: Somatic Variant Caller (Illumina) and Mutect2 (GATK version 4.0.3) and potential driver mutations were predicted according to previously published criteria.⁵ SIFT predictor was only used for mutations in which a definitive score was not provided by Mutation Assessor.



Supplementary Tables

Supplementary Table S1. Details of all antibodies used, source and conditions of use.

Antibody	Clone	Source	Antigen retrieval/visualization	Dilution
CD20	L26	DAKO, Copenhagen, Denmark	EDTA 1 mM pH 9/ ENVISION FLEX (DAKO)	RTU
CD79a	JCB 117	DAKO	EDTA 1 mM pH 9/ ENVISION FLEX (DAKO)	RTU
CD3	Polyclonal	DAKO	EDTA 1 mM pH 9/ ENVISION FLEX (DAKO)	RTU
CD5	4C7	DAKO	EDTA 1 mM pH 9/ ENVISION FLEX (DAKO)	RTU
CD10	56C6	DAKO	EDTA 1 mM pH 9/ ENVISION FLEX (DAKO)	RTU
BCL6	PG-B6p	DAKO	EDTA 1 mM pH 9/ ENVISION FLEX (DAKO)	RTU
BCL2	124	DAKO	EDTA 1 mM pH 9/ ENVISION FLEX (DAKO)	RTU
Ki67	Mib-1	DAKO	Citrate 10 mM pH 6/ ENVISION FLEX (DAKO)	RTU
MUM1	MRQ-43	Ventana, Roche	CC1 solution / ultraView Universal DAB Detection Kit. Automated immunostainer (Benchmark XT; Ventana)	RTU
MYC*	Y69	Ventana, Roche	CC1 solution / ultraView Universal DAB Detection Kit. Automated immunostainer (Benchmark XT; Ventana)	RTU
LMO2*	1A9-1	Ventana, Roche, Tucson, AZ,USA	CC1 solution / ultraView Universal DAB Detection Kit. Automated immunostainer (Benchmark XT; Ventana)	RTU

RTU, ready to use.

*LMO2 was considered positive when >30% of the cells were positive and MYC was considered positive when more than 40% of positive tumor cells were observed, following the criteria of Colomo et al¹⁷ and Johnson et al respectively.¹⁸

Supplementary Table S2. Ninety-six genes sequenced using Target NGS panel including references for inclusion in the mutational analysis and mean coverage by gene and amplicon.

Provided in excel format

Supplementary Table S3. Primers used for the verification of variants in *MYC*, *BTG2*, *ETS1* and *TP53* and the re-analysis of *ID3*, *TCF3* (exon 17) and *CCND3* (exon 5).

Primers <i>ETS1</i>					
Primer	Sequence (5'-3')	PCR product length (bp)	Case/Mutation	Variant	Mutation position (hg19)
ETS1_1 F	CTGCAGGTCACACACAAAGC	157	BLL2	T>T/C	128332392
ETS1_1 R	TAAATTTTCAGGTGGCCAGGA		BLL7	C>C/T	128332410
ETS1_5 F	CCACGGCTCAGTTTCTCATA	168	BLL2	A>A/T	128332477
ETS1_5 R	GGGTCACCATGAATGGGTAT				
ETS1_3 F	TTTGAATCCCAGCCATCTC	167	BLL14	G>G/A	128333508
ETS1_3 F	GTGGGGATTAGCTGCGTAGA				
ETS1_E1F	GAAAGGGGGAAGAAGTCCAG	200	Exon 1 of transcript M_005238		
ETS1_E1R	CAAACCTTGCTACCATCCCGTA				

Primers <i>BTG2</i>					
Primer	Sequence (5'-3')	PCR product length (bp)	Case/Mutation	Variant	Mutation position (hg19)
BTG2_1F	GACATGAGCCACGGGAAG	228	BLL1	C>C/T	203274858
BTG2_1R	CTGCCGCAGGAGTAGAAGAA		BLL2	G>G/A	203274867
			BLL7	del	203274878

Primers <i>MYC</i>					
Primer	Sequence (5'-3')	PCR product length (bp)	Case/Mutation	Variant	Mutation position (hg19)
MYC_2 F	GAGCTGCTGGGAGGAGACAT	150	BLL7	T>T/G	128750921
MYC_2 R	CTGGTAGGAGGCCAGCTTCT				
MYC_4 F	CTCCTGGCAAAAGGTCAGAG	158	BLL1	C>C/G	128752800
MYC_4 R	CCTCTTGGCAGCAGGATAGT				

Primers <i>TP53</i>					
Primer	Sequence (5'-3')	PCR product length (bp)	Case/Mutation	Variant	Mutation position (hg19)
TP53_2 F	CCAGTGTGATGATGGTGAGG	163	BLL4	C>C/T	7577538
TP53_2 R	CCTGCTTGCCACAGGTCT				

Primers <i>ID3</i>			
Primer	Sequence (5'-3')	PCR product length (bp)	Reference

ID3-FZ-F	TCCAGGCAGGCTCTATAAGTG	694	Rohde, et al ¹⁹
ID3-FZ-R	CCGAGTGAGTGGCAATTTT		Rohde, et al ¹⁹
ID3-PE-F	GCTTACCTGGATGGGAAGGT	204	
ID3-PE-R	GAGGAGCCGCTGAGCTTG		

Primers <i>TCF3</i>			
Primer	Sequence (5'-3')	PCR product length (bp)	Reference

TCF3-FZ-F	TGCTGTGCCACCAATGTAAG CCATG	609	Rohde, et al ¹⁹
TCF3-FZ-R	GTGGAGGCTTGTAAGAAGAG AGTGG		Rohde, et al ¹⁹
TCF3-PE-F	CAGGATGAGCAGCTTGGTCT	180	
TCF3-PE-R	AGTACGGACGAGGTGCTGTC		

Primers <i>CCND3</i>			
Primer	Sequence (5'-3')	PCR product length (bp)	Reference

CCND3-FZ-F	CCATGTGTTGGGAGCTGTC	328	Rohde, et al ¹⁹
CCND3-FZ-R	CTGGAGGCAGGGAGGTG		Rohde, et al ¹⁹
CCND3-PE-F	GCCCCTCCTCTGCTTAGTG	198	
CCND3-PE-R	CTGTCAGGAGCAGATCGAAG		

Bp: base pairs; F: forward, R: reverse

Supplementary Table S4. Taqman assays used for qPCR analyses. (Applied Biosystems inc)

Gene Symbol	Assay ID	Amplicon size (bp)	Reference sequence
<i>ETS1</i>	Hs00428293_m1	99	NM_005238
<i>MYC</i>	Hs00153408_m1	107	NM_002467
<i>B2M</i>	Hs00984230_m1	81	NM_004048

Supplementary Table S5. Summary of copy number findings and FISH pattern constellation of the 11q aberration in the current series of BLL-11q.

Case	CN array		11q FISH (CEP11 [D11Z1] + RP11-414G21+RP11-629A20)	
	Pattern of chr11	Number of alterations	11q FISH constellation pattern ²⁰	11q FISH result
#1	Only terminal loss	2 CNA	nuc ish (D11Z1x2,RP11-414G21x2,RP11-629A20x1)	Only terminal loss
#2	Gain/terminal loss	3 CNA	nuc ish (D11Z1x2,RP11-414G21x2,RP11-629A20x1)	Only terminal loss
#3	Gain/terminal loss	6 CNA, 1 CNN-LOH	nuc ish (D11Z1x2,RP11-414G21x2-3,RP11-629A20x1)	Gain*/terminal loss
#4	Gain/amplification/CNN-LOH	15 CNA+ 1CNN-LOH	nuc ish (D11Z1x2,RP11-414G21x2-5,RP11-629A20x2)	Amplification
#5	Gain/amplification/terminal loss	4 CNA	nuc ish (D11Z1x2,RP11-414G21x4-5,RP11-629A20x1)	Amplification/terminal loss
#6	Only terminal loss	6 CNA + 11 CNN-LOH	nuc ish (D11Z1x2,RP11-414G21x2,RP11-629A20x1)	Only terminal loss
#7	Gain/terminal loss	8 CNA	nuc ish (D11Z1x2,RP11-414G21x3,RP11-629A20x1)	Gain/terminal loss
#14	Gain/terminal loss	4 CNA	nuc ish (D11Z1x2,RP11-414G21x2,RP11-629A20x1)	Only terminal loss
#15	Gain/terminal loss	12 CNA + 1CNN-LOH	Not done	
#16	Gain/amplification/terminal loss	4 CNA	nuc ish (D11Z1x2,RP11-414G21x3,RP11-629A20x1)	Gain/terminal loss
#17	Gain/amplification/terminal loss	14 CNA +3 CNN-LOH	nuc ish (D11Z1x2,RP11-414G21x3-4,RP11-629A20x1)	Amplification*/terminal loss

CNA: copy number alteration. CNN-LOH: copy number neutral loss of heterozygosity. *Only observed in a few cells. CN and FISH results were not concordant in cases #2, and #14 most likely due to the fact that gained region covered by BAC RP11-414G21 was most likely inverted and then both copies were very narrow to be clearly distinguished as independent signals in the FISH constellation.

Supplementary Table S6. Global table of copy number and copy number neutral of heterozygosity (CNN-LOH) alterations of the 11 BLL-11q aberration and the 6 MYC-negative 11q-negative cases.

Case	Array	Chromosome Region (Hg19)	Event	Length (bp)	Cytoband
#1					
	Oncoscan	chr6:67,759,432-110,118,776	CN Loss	42359345	q12 - q21
	Oncoscan	chr11:124,440,617-132,877,670	CN Loss	8437054	q24.2 - q25
#2					
	Cytoscan	chr6:302,273-3,157,193	CN Gain	2854921	p25.3 - p25.2
	Cytoscan	chr11:66,015,813-120,252,657	CN Gain	54236845	q13.2 - q23.3
	Cytoscan	chr11:120,253,875-135,006,516	CN Loss	14752642	q23.3 - q25
#3					
	Oncoscan	chr5:1-180,915,260	CN Gain	180915260	p15.33 - q35.3
	Oncoscan	chr11:103,326,831-111,737,912	CN Gain	8411082	q22.3 - q23.1
	Oncoscan	chr11:111,747,297-113,562,039	CN Loss	1814743	q23.1 - q23.2
	Oncoscan	chr11:114,767,237-116,764,582	CN Gain	1997346	q23.3
	Oncoscan	chr11:127,681,132-132,020,453	CN Loss	4339322	q24.2 - q25
	Oncoscan	chr17:40,114,049-81,195,210	CNN-LOH	41081162	q21.2 - q25.3
	Oncoscan	chr18:20,935,833-78,007,784	CN Gain	57071952	q11.2 - q23
#4					
	SNP6	chr3:148,377,370-198,022,430	CN Gain	49645061	q24 - q29
	SNP6	chr4:151,106,726-151,889,624	CN Loss	782899	q31.3
	SNP6	chr6:62,787,661-63,773,155	CN Loss	985495	q11.1 - q12
	SNP6	chr6:66,807,178-136,034,966	CN Loss	69227789	q12 - q23.3
	SNP6	chr6:137,582,049-168,332,407	CN Loss	30750359	q23.3 - q27
	SNP6	chr6:168,596,580-171,115,067	CN Loss	2518488	q27
	SNP6	chr8:118,905,307-134,171,629	CN Gain	15266323	q24.11 - q24.22
	SNP6	chr11:77,429,089-117,851,837	CN Gain	40422749	q14.1 - q23.3
	SNP6	chr11:117,851,837-120,155,799	High Copy Gain	2303963	q23.3
	SNP6	chr11:120,155,799-135,006,516	CNN-LOH	14850718	q23.3 - q25
	SNP6	chr12:40,494,911-93,085,645	CN Gain	52590735	q12 - q22
	SNP6	chr12:93,085,646-95,374,851	CN Loss	2289206	q22
	SNP6	chr12:95,374,851-96,373,225	CN Gain	998375	q22 - q23.1
	SNP6	chr18:29,031,540-56,749,287	CN Gain	27717748	q12.1 - q21.32
	SNP6	chr18:56,749,288-78,077,248	CN Loss	21327961	q21.32 - q23
	SNP6	chr19:6,700,469-6,935,092	CN Loss	234624	p13.3 - p13.2

Case	Array	Chromosome Region (Hg19)	Event	Length (bp)	Cytoband
#5					
	Oncoscan	chr6:78,975,348-114,942,024	CN Loss	35966677	q14.1 - q22.1
	Oncoscan	chr11:83,088,730-117,240,357	CN Gain	34151628	q14.1 - q23.3
	Oncoscan	chr11:117,242,677-120,392,430	High Copy Gain	3149754	q23.3
	Oncoscan	chr11:120,398,613-134,938,847	CN Loss	14540235	q23.3 - q25
#6					
	Oncoscan	chr1:150,029,936-151,599,267	High Copy Gain	1569332	q21.2 - q21.3
	Oncoscan	chr1:151,744,168-249,212,878	CNN-LOH	97468711	q21.3 - q44
	Oncoscan	chr3:117,248,700-124,701,188	CNN-LOH	7452489	q13.31 - q21.2
	Oncoscan	chr3:177,647,728-197,852,564	CN Gain	20204837	q26.32 - q29
	Oncoscan	chr4:124,989,820-147,017,448	CNN-LOH	22027629	q28.1 - q31.22
	Oncoscan	chr5:38,139-5,124,613	CNN-LOH	5086475	p15.33 - p15.32
	Oncoscan	chr5:76,061,256-96,465,623	CNN-LOH	20404368	q13.3 - q15
	Oncoscan	chr5:171,201,195-180,698,312	CNN-LOH	9497118	q35.1 - q35.3
	Oncoscan	chr8:79,796,337-94,671,697	CNN-LOH	14875361	q21.12 - q22.1
	Oncoscan	chr9:204,738-10,275,857	CNN-LOH	10071120	p24.3 - p23
	Oncoscan	chr11:70,045,922-106,288,554	CNN-LOH	36242633	q13.3 - q22.3
	Oncoscan	chr11:128,214,400-134,938,847	CN Loss	6724448	q24.3 - q25
	Oncoscan	chr12:189,400-133,818,115	CN Gain	133628716	p13.33 - q24.33
	Oncoscan	chr13:91,639,578-92,147,712	CN Gain	508135	q31.3
	Oncoscan	chr14:54,084,642-76,110,632	CNN-LOH	22025991	q22.1 - q24.3
	Oncoscan	chr18:59,650,717-62,178,511	CN Gain	2527795	q21.33 - q22.1
	Oncoscan	chr18:55,902,055-66,218,776	CNN-LOH	10316722	q21.31 - q22.1
#7					
	Cytoscan	chr1:5,195,097-7,019,203	CN Loss	1824107	p36.32 - p36.31
	Cytoscan	chr3:60,388,322-60,712,277	CN Loss	323956	p14.2
	Cytoscan	chr5:104,762,975-174,135,222	CN Gain	69372248	q21.3 - q35.2
	Cytoscan	chr5:178,688,093-180,719,789	CN Gain	2031697	q35.3
	Cytoscan	chr11:72,390,640-72,717,317	High Copy Gain	326678	q13.4
	Cytoscan	chr11:72,717,332-119,682,209	CN Gain	46964878	q13.4 - q23.3
	Cytoscan	chr11:119,682,255-134,938,470	CN Loss	15256216	q23.3 - q25
	Cytoscan	chr12:1-133,851,895	CN Gain	133851895	p13.33 - q24.33

Case	Array	Chromosome Region (Hg19)	Event	Length (bp)	Cytoband
#8					
	Oncoscan	chr1:23,506,625-23,985,309	CN Loss	478685	p36.12 - p36.11
	Oncoscan	chr1:116,776,586-118,300,350	CN Loss	1523765	p13.1 - p12
	Oncoscan	chr1:189,763,755-200,583,380	CN Gain	10819626	q31.1 - q32.1
	Oncoscan	chr2:180,790,820-198,749,269	CN Gain	17958450	q31.3 - q33.1
	Oncoscan	chr6:204,909-57,305,822	CN Gain	57100914	p25.3 - p11.2
	Oncoscan	chr6:57,329,886-58,055,927	CN Loss	726042	p11.2
	Oncoscan	chr6:58,213,475-58,770,502	CN Gain	557028	p11.2 - p11.1
	Oncoscan	chr6:61,886,393-170,913,051	CN Loss	109026659	q11.1 - q27
	Oncoscan	chr7:1-159,138,663	CN Gain	159138663	p22.3 - q36.3
	Oncoscan	chr7:1-159,138,663	CNN-LOH	159138663	p22.3 - q36.3
	Oncoscan	chr8:55,457,188-71,067,368	CN Loss	15610181	q11.23 - q13.3
	Oncoscan	chr9:204,738-35,809,328	CNN-LOH	35604591	p24.3 - p13.3
	Oncoscan	chr9:21,901,263-22,056,499	Homozygous Copy Loss	155237	p21.3
	Oncoscan	chr11:45,810,652-46,460,038	CN Loss	649387	p11.2
	Oncoscan	chr12:189,400-8,447,618	CN Loss	8258219	p13.33 - p13.31
	Oncoscan	chr12:19,557,354-21,282,570	CN Loss	1725217	p12.3 - p12.2
	Oncoscan	chr12:21,295,612-29,285,577	CN Gain	7989966	p12.2 - p11.22
	Oncoscan	chr12:30,814,259-33,886,138	CN Gain	3071880	p11.21 - p11.1
	Oncoscan	chr12:39,204,714-70,880,468	CN Gain	31675755	q12 - q15
	Oncoscan	chr12:74,309,125-77,911,802	CN Gain	3602678	q21.1 - q21.2
	Oncoscan	chr12:79,610,263-82,677,229	CN Gain	3066967	q21.2 - q21.31
	Oncoscan	chr12:84,462,140-89,275,759	CN Loss	4813620	q21.31 - q21.33
	Oncoscan	chr12:91,825,095-94,371,476	CN Loss	2546382	q21.33 - q22
	Oncoscan	chr12:98,498,625-115,061,325	CN Gain	16562701	q23.1 - q24.21
	Oncoscan	chr12:128,397,472-133,818,115	CN Gain	5420644	q24.32 - q24.33
	Oncoscan	chr13:45,901,876-53,198,648	CN Loss	7296773	q14.13 - q14.3
	Oncoscan	chr13:58,291,792-69,716,364	CN Gain	11424573	q21.1 - q21.33
	Oncoscan	chr20:29,519,156-40,272,376	CN Loss	10753221	q11.21 - q12
	Oncoscan	chrX:1-155,270,560	CN Loss	155270560	p22.33 - q28
#9					
	Oncoscan	chr5:1-180,915,260	CN Gain	180915260	p15.33 - q35.3
	Oncoscan	chr6:204,909-52,036,300	CNN-LOH	51831392	p25.3 - p12.2
	Oncoscan	chr6:32,100,302-32,998,152	High Copy Gain	897851	p21.32
	Oncoscan	chr7:41,421-159,118,443	CN Gain	159077023	p22.3 - q36.3
	Oncoscan	chr12:1-133,851,895	CN Gain	133851895	p13.33 - q24.33
	Oncoscan	chr17:40,424,255-80,263,427	CNN-LOH	39839173	q21.2 - q25.3
	Oncoscan	chr17:62,949,100-63,165,077	Homozygous Copy Loss	215978	q24.1
	Oncoscan	chr21:14,375,361-48,045,085	CN Gain	33669725	q11.2 - q22.3

Case	Array	Chromosome Region (Hg19)	Event	Length (bp)	Cytoband
#10					
	Oncoscan	chr17:400,959-12,159,990	CNN-LOH	11759032	p13.3 - p12
#11					
	SNP6	chr1:73,100,845-74,442,581	CN Gain	1341737	p31.1
	SNP6	chr1:149,962,792-152,551,299	CN Gain	2588508	q21.2 - q21.3
	SNP6	chr6:40,083,170-42,855,926	CN Gain	2772757	p21.2 - p21.1
	SNP6	chr6:78,166,644-117,921,913	CN Loss	39755270	q14.1 - q22.1
	SNP6	chr8:106,741,322-107,876,319	CN Gain	1134998	q23.1
	SNP6	chr8:128,951,273-129,358,847	CN Gain	407575	q24.21
	SNP6	chr9:223,542-3,003,015	CN Gain	2779474	p24.3 - p24.2
	SNP6	chr12:0-133,851,895	CN Gain	133851896	p13.33 - q24.33
	SNP6	chr13:56,118,024-57,280,068	CN Gain	1162045	q21.1
	SNP6	chr13:91,986,235-92,361,312	CN Gain	375078	q31.3
	SNP6	chr17:49,745,106-81,195,210	CNN-LOH	31450105	q21.33 - q25.3
	SNP6	chr19:1-12,492,039	CNN-LOH	12492039	p13.3 - p13.2
	SNP6	chr19:6,493,673-7,463,666	Homozygous Copy Loss	969994	p13.3 - p13.2
	SNP6	chr19:37,006,258-37,414,445	CN Loss	408188	q13.12
	SNP6	chr21:14,369,207-48,129,895	CN Gain	33760689	q11.2 - q22.3
#12					
	Oncoscan	chr1:144,790,037-193,932,788	CN Gain	49142752	q21.1 - q31.3
	Oncoscan	chr2:134,242,471-139,641,542	CN Gain	5399072	q21.2 - q22.1
	Oncoscan	chr2:212,437,072-215,227,024	CN Gain	2789953	q34
	Oncoscan	chr3:63,411-60,777,554	CNN-LOH	60714144	p26.3 - p14.2
	Oncoscan	chr3:116,120,738-117,045,461	CN Loss	924724	q13.31
	Oncoscan	chr4:181,713,895-190,915,650	CN Loss	9201756	q34.3 - q35.2
	Oncoscan	chr5:38,139-1,985,845	CN Gain	1947707	p15.33
	Oncoscan	chr6:85,053,988-92,677,362	CN Gain	7623375	q14.3 - q15
	Oncoscan	chr7:88,362,639-94,444,750	CN Gain	6082112	q21.13 - q21.3
	Oncoscan	chr8:128,651,315-128,766,080	CN Gain	114766	q24.21
	Oncoscan	chr8:128,767,004-128,840,276	CN Loss	73273	q24.21
	Oncoscan	chr13:64,574,475-69,315,335	CN Gain	4740861	q21.31 - q21.33
	Oncoscan	chr17:400,959-19,497,890	CNN-LOH	19096932	p13.3 - p11.2
	Oncoscan	chr19:247,232-3,093,163	CN Gain	2845932	p13.3
	Oncoscan	chr22:42,109,917-51,213,826	CN Loss	9103910	q13.2 - q13.33

Case	Array	Chromosome Region (Hg19)	Event	Length (bp)	Cytoband
#13					
	Oncoscan	chr7:41,421-24,971,213	CN Gain	24929793	p22.3 - p15.3
	Oncoscan	chrX:25,296,129-58,470,802	CN Gain	33174674	p21.3 - p11.1
	Oncoscan	chr10:567,325-135,434,303	CN Gain	134866979	p15.3 - q26.3
	Oncoscan	chr4:91,749,811-91,794,821	CN Gain	45011	q22.1
	Oncoscan	chr1:104,446,681-110,195,901	CN Gain	5749221	p21.1 - p13.3
	Oncoscan	chr1:110,200,360-110,240,929	CN Gain	40570	p13.3
	Oncoscan	chr12:189,400-133,818,115	CN Gain	133628716	p13.33 - q24.33
	Oncoscan	chr2:32,757,598-37,578,208	CN Loss	4820611	p22.3 - p22.2
	Oncoscan	chr2:121,588,532-129,317,105	CN Loss	7728574	q14.2 - q14.3
	Oncoscan	chr2:137,910,175-151,016,074	CN Loss	13105900	q22.1 - q23.3
	Oncoscan	chr2:153,153,555-160,994,348	CN Loss	7840794	q23.3 - q24.2
	Oncoscan	chr19:247,232-11,674,294	CNN-LOH	11427063	p13.3 - p13.2
	Oncoscan	chr19:6,528,235-7,104,673	Homozygous Copy Loss	576439	p13.3 - p13.2
#14					
	Oncoscan	chr7:74,132,398-159,118,443	CN Gain	84986046	q11.23 - q36.3
	Oncoscan	chr11:1-60,760,530	CN Gain	60760530	p15.5 - q12.2
	Oncoscan	chr11:91,274,842-118,350,945	CN Gain	27076104	q14.3 - q23.3
	Oncoscan	chr11:118,352,769-134,938,847	CN Loss	16586079	q23.3 - q25
#15					
	Oncoscan	chr5:99,257,992-146,632,594	CN Gain	47374603	q21.1 - q32
	Oncoscan	chr6:63,365,565-123,492,278	CN Loss	60126714	q11.2 - q22.31
	Oncoscan	chr10:122,564,306-135,434,303	CN Gain	12869998	q26.12 - q26.3
	Oncoscan	chr11:93,515,058-120,717,000	CN Gain	27201943	q21 - q23.3
	Oncoscan	chr11:120,732,508-135,006,516	CN Loss	14274009	q23.3 - q25
	Oncoscan	chr12:189,400-1,896,956	CN Gain	1707557	p13.33
	Oncoscan	chr12:22,812,766-28,466,571	High Copy Gain	5653806	p12.1 - p11.22
	Oncoscan	chr12:28,476,847-64,720,693	CN Gain	36243847	p11.22 - q14.2
	Oncoscan	chr12:64,720,694-73,671,118	High Copy Gain	8950425	q14.2 - q21.1
	Oncoscan	chr13:85,803,897-99,955,533	CN Gain	14151637	q31.1 - q32.3
	Oncoscan	chr13:99,967,798-115,103,150	CN Loss	15135353	q32.3 - q34
	Oncoscan	chr16:58,143,392-90,195,538	CN Gain	32052147	q21 - q24.3
	Oncoscan	chr17:59,315,145-80,263,427	CNN-LOH	20948283	q23.2 - q25.3
#16					
	Oncoscan	chr6:83,574,391-120,108,162	CN Loss	36533772	q14.1 - q22.31
	Oncoscan	chr11:73,228,685-113,724,673	CN Gain	40495989	q13.4 - q23.2
	Oncoscan	chr11:113,733,111-120,176,979	High Copy Gain	6443869	q23.2 - q23.3
	Oncoscan	chr11:120,187,433-134,938,847	CN Loss	14751415	q23.3 - q25

Case	Array	Chromosome Region (Hg19)	Event	Length (bp)	Cytoband
#17					
	Oncoscan	chr3:149,230,137-197,852,564	CN Gain	48622428	q25.1 - q29
	Oncoscan	chr4:77,277,624-107,631,213	CN Gain	30353590	q21.1 - q24
	Oncoscan	chr7:111,092,478-159,118,443	CN Loss	48025966	q31.1 - q36.3
	Oncoscan	chr8:172,417-33,010,693	CNN-LOH	32838277	p23.3 - p12
	Oncoscan	chr8:1-146,364,022	CN Gain	146364022	p23.3 - q24.3
	Oncoscan	chr8:58,406,216-146,292,734	CNN-LOH	87886519	q12.1 - q24.3
	Oncoscan	chr11:70,719,897-118,343,378	CN Gain	47623482	q13.4 - q23.3
	Oncoscan	chr11:118,347,020-121,053,084	High Copy Gain	2706065	q23.3
	Oncoscan	chr11:121,062,860-134,906,706	CN Loss	13843847	q23.3 - q25
	Oncoscan	chr13:79,420,211-83,071,814	High Copy Gain	3651604	q31.1
	Oncoscan	chr13:83,098,518-94,240,082	CN Gain	11141565	q31.1 - q31.3
	Oncoscan	chr13:94,251,808-115,103,150	CN Loss	20851343	q31.3 - q34
	Oncoscan	chr15:74,343,354-102,397,317	CN Gain	28053964	q24.1 - q26.3
	Oncoscan	chr17:7,536,527-7,619,668	CN Loss	83142	p13.1
	Oncoscan	chr18:33,243,441-55,865,613	CN Gain	22622173	q12.2 - q21.31
	Oncoscan	chr18:55,893,217-78,007,784	CN Loss	22114568	q21.31 - q23
	Oncoscan	chr20:32,385,089-62,912,463	CNN-LOH	30527375	q11.22 - q13.33

Supplementary Table S7. List of somatic mutations in BLL-11q including prediction of amino acid changes that affect protein function (MA, SIFT, Polyphen2, CADD).

Provided in excel format.

Supplementary Table S8. Mutational patterns across different germinal center derived lymphoma subgroups including BL,^{21,22} DLBCL,^{5,23} DH/TH,^{24,25} and HGBCL, NOS with or without *MYC* rearrangement.²⁵ The BL pattern includes mutations in BL-associated genes and the GCB-DLBCL pattern includes mutations associated with GCB phenotype according to literature. BLL-11q mutational pattern includes genes mutated in more than 2 BLL-11q cases, not included in the other two signatures.

Mutational patterns	Gene	BLL-11q current series n=10 (%)	GCB-DLBCL n=83 (%)	HGBCL DH/TH n=44 (%)	HGBCL with or without <i>MYC</i> -R n=9 (%)	BL n=32 (%)
BLL-11q	<i>BTG2</i>	40	4.8*	-	-	0*
	<i>ETS1</i>	30	1.2*	-	-	0*
	<i>EP300</i>	30	6*	6.8	0	0*
Burkitt Lymphoma	<i>ID3</i>	0	0	25	88.9*	59.4*
	<i>TCF3</i>	0	0	4.5	0	31.3
	<i>CCND3</i>	0	3,6	29.2 ^b	22.2	9.4
	<i>MYC</i>	20	2.4	43.2	44.4	71.9*
	<i>DDX3X</i>	30	0 ^a *	-	-	31.3
GCB-DLBCL	<i>KMT2D</i>	20	32.5	60 ^c	-	6.3
	<i>CREBBP</i>	20	25.3	50	44.4	6.3
	<i>TNFRSF14</i>	0	20.5	20 ^c	-	0
	<i>B2M</i>	0	20.5	10 ^c	-	0
	<i>EZH2</i>	10	21.7	27.3	0	0
	<i>GNA13</i>	30	21.7	15 ^c	-	9.4
	<i>FOXO1</i>	10	13.3	30 ^c	-	6.3
	<i>ACTB</i>	0	13.3	-	-	0
<i>SOCS1</i>	0	15.7	30 ^c	-	0	

* Significant differences of mutated gene prevalence between BLL-11q series and the other germinal center entities ($P < 0.05$).

^a Only in Morin et al series n=23. ^b Only in Momose et al. n=24. ^c Only in Evrard et al. n=20.

Supplementary References

1. Scholtysik R, Kreuz M, Klapper W et al. Detection of genomic aberrations in molecularly defined Burkitt's lymphoma by array-based, high resolution, single nucleotide polymorphism analysis. *Haematologica*. 2010;95(12):2047-2055.
2. Li H, Durbin R. Fast and accurate short read alignment with Burrows-Wheeler transform. *Bioinformatics*. 2009;25(14):1754-1760.
3. McKenna A, Hanna M, Banks E et al. The Genome Analysis Toolkit: a MapReduce framework for analyzing next-generation DNA sequencing data. *Genome Res*. 2010;20(9):1297-1303.
4. Wang K, Li M, Hakonarson H. ANNOVAR: functional annotation of genetic variants from high-throughput sequencing data. *Nucleic Acids Res*. 2010;38(16):e164.
5. Karube K, Enjuanes A, Dlouhy I et al. Integrating genomic alterations in diffuse large B-cell lymphoma identifies new relevant pathways and potential therapeutic targets. *Leukemia*. 2018;32(3):675-684.
6. Reva B, Antipin Y, Sander C. Predicting the functional impact of protein mutations: application to cancer genomics. *Nucleic Acids Res*. 2011;39(17):e118.
7. Kumar P, Henikoff S, Ng PC. Predicting the effects of coding non-synonymous variants on protein function using the SIFT algorithm. *Nat Protoc*. 2009;4(7):1073-1081.
8. Adzhubei IA, Schmidt S, Peshkin L et al. A method and server for predicting damaging missense mutations. *Nat Methods*. 2010;7(4):248-249.
9. Kircher M, Witten DM, Jain P et al. A general framework for estimating the relative pathogenicity of human genetic variants. *Nat Genet*. 2014;46(3):310-315.
10. Salaverria I, Royo C, Carvajal-Cuenca A et al. CCND2 rearrangements are the most frequent genetic events in cyclin D1(-) mantle cell lymphoma. *Blood*. 2013;121(8):1394-1402.
11. Bouska A, McKeithan TW, Deffenbacher KE et al. Genome-wide copy-number analyses reveal genomic abnormalities involved in transformation of follicular lymphoma. *Blood*. 2014;123(11):1681-1690.
12. Spina V, Khiabani H, Messina M et al. The genetics of nodal marginal zone lymphoma. *Blood*. 2016;128(10):1362-1373.
13. Puente XS, Bea S, Valdes-Mas R et al. Non-coding recurrent mutations in chronic lymphocytic leukaemia. *Nature*. 2015;526(7574):519-24.
14. Lopez-Corral L, Sarasquete ME, Bea S et al. SNP-based mapping arrays reveal high genomic complexity in monoclonal gammopathies, from MGUS to myeloma status. *Leukemia*. 2012;26(12):2521-2529.
15. Paiva B, Mateos MV, Sanchez-Abarca LI et al. Immune status of high-risk smoldering multiple myeloma patients and its therapeutic modulation under LenDex: a longitudinal analysis. *Blood*. 2016;127(9):1151-1162.
16. Swerdlow SH, Campo E, Harris NL, Jaffe ES, Pileri SA, Stein H, Thiele J (Eds) WHO Classification of Tumours of Haematopoietic and Lymphoid Tissues. (Revised 4th edition) IARC: Lyon 2017.
17. Colomo L, Vazquez I, Papaleo N et al. LMO2-negative Expression Predicts the Presence of MYC Translocations in Aggressive B-Cell Lymphomas. *Am J Surg Pathol*. 2017;41(7):877-886.

18. Johnson NA, Slack GW, Savage KJ et al. Concurrent expression of MYC and BCL2 in diffuse large B-cell lymphoma treated with rituximab plus cyclophosphamide, doxorubicin, vincristine, and prednisone. *J Clin Oncol*. 2012;30(28):3452-3459.
19. Rohde M, Bonn BR, Zimmermann M et al. Relevance of ID3-TCF3-CCND3 pathway mutations in pediatric aggressive B-cell lymphoma treated according to the non-Hodgkin Lymphoma Berlin-Frankfurt-Munster protocols. *Haematologica*. 2017;102(6):1091-1098.
20. ISCN 2013: an international system for human cytogenetic nomenclature (2013). In: Shaffer Lisa G., McGowan-Jordan J, Schmid M, eds.: Karger; 2013.
21. Schmitz R, Young RM, Ceribelli M et al. Burkitt lymphoma pathogenesis and therapeutic targets from structural and functional genomics. *Nature*. 2012;490(7418):116-120.
22. Richter J, Schlesner M, Hoffmann S et al. Recurrent mutation of the ID3 gene in Burkitt lymphoma identified by integrated genome, exome and transcriptome sequencing. *Nat Genet*. 2012;44(12):1316-1320.
23. Morin RD, Mungall K, Pleasance E et al. Mutational and structural analysis of diffuse large B-cell lymphoma using whole-genome sequencing. *Blood*. 2013;122(7):1256-1265.
24. Evrard SM, Pericart S, Grand D et al. Targeted next generation sequencing reveals high mutation frequency of CREBBP, BCL2 and KMT2D in high-grade B-cell lymphoma with MYC and BCL2 and /or BCL6 rearrangements. *Haematologica*. 2018
25. Momose S, Weissbach S, Pischmarov J et al. The diagnostic gray zone between Burkitt lymphoma and diffuse large B-cell lymphoma is also a gray zone of the mutational spectrum. *Leukemia*. 2015;29(8):1789-1791.